
“Semiconductor” Model of the “Polymer-CNTs” Composite Strengthening

Karachevtseva Liudmyla^{1,2,*}, Kartel Mykola^{1,3}, Wang Bo¹, Lytvynenko Oleg², Onyshchenko Volodymyr², Sementsov Yurii^{1,3}, Trachevskiy Viacheslav¹

¹Technology and Business Department, Ningbo University of Technology, Ningbo, China

²Department of Photonic Crystals, V. Lashkaryov Institute of Semiconductor Physics, NAS of Ukraine, Kyiv, Ukraine

³Department of Carbon Nanomaterials, O. Chuiko Institute of Surface Chemistry, NAS of Ukraine, Kyiv, Ukraine

Email address:

lakar@isp.kiev.ua (K. Liudmyla), nikar@kartel.kiev.ua (K. Mykola)

*Corresponding author

To cite this article:

Karachevtseva Liudmyla, Kartel Mykola, Wang Bo, Lytvynenko Oleg, Onyshchenko Volodymyr, Sementsov Yurii, Trachevskiy Viacheslav. “Semiconductor” Model of the “Polymer-CNTs” Composite Strengthening. *International Journal of Materials Science and Applications*. Vol. 8, No. 6, 2019, pp. 120-126. doi: 10.11648/j.ijmsa.20190806.15

Received: August 20, 2019; **Accepted:** October 20, 2019; **Published:** December 3, 2019

Abstract: We analyzed “semiconductor” model of the “polymer-CNTs” composite strengthening at 300 K and low (0.1-0.5) wt% CNTs concentration. Carbon nanotubes are among the most anisotropic materials known and have extremely high values of Young's modulus. We investigated influence of vibration bonds on polymer crystallization and strengthening in composite films of polyethylenimine, polyamide, polypropylene and rubber with multiwall carbon nanotubes. IR absorbance maxima we evaluated after formation of composite “polyethylenimine-carbon nanotube” in the spectral area of the sp^3 hybridization bonds at the frequency of primary amino groups of polyethylenimine. High IR absorption in the spectral area of sp^3 hybridization bonds of polypropylene, polyamide-6 with carbon nanotubes is determined by $\gamma_{\omega}(\text{CH})$ and $\gamma_{\omega}(\text{CH}_2)$ vibrations. We measured IR reflectance maxima of composite “rubber-carbon nanotube” in the spectral area of CH valence and deformation vibrations. The IR peak dependence on the carbon nanotube content corresponds to 1D Gaussian curve for the diffusion equation in the electric field between electrons of nanotubes and protons in polymer according to “semiconductor” model of the composite structuring. For our case of the long-acting hundreds nanometer interactions, the polymer crystallization depends on sp^3 C-C bonds organization in the intrinsic electric field according to the semiconductor n-p model. Tensile strength for polyamide-6 composites at 0.25% CNTs increases 1.7 times and tensile deformation – 2.3 times.

Keywords: Polymer Composites, Multiwall Carbon Nanotubes, Electric Field

1. Introduction

Multiwall carbon nanotubes are among the most anisotropic materials known and have extremely high values of Young's modulus [1]. Carbon nanotube aspect ratio of length to diameter is more than 10^3 ; this distinguishes it from other nanoparticles. New composites with carbon nanotubes (CNTs) as additives were studied intensively during the last decade. Composites are characterized by extremely high specific strength properties [2], electrical and thermal conductivity [3]. The presence of CNT in the matrix improves the composite biocompatibility [4]. CNTs exhibit both semiconducting and metallic behavior depending on

their chirality [5]. Researchers have successfully demonstrated field-effect transistors based on semiconducting CNTs [6]. Metallic CNTs have been considered as a potential solution for on-chip interconnects with a current density well above 10^6 A/cm² [7]. The connection of CNTs to silicon has been realized, using polyethylenimine (PEI) as a binding material between them [8]. Chemical hydrogen bonding and electrostatic interaction between PEI, CNTs, and silicon effectively connect CNTs to silicon. Electric transport at this junction shows a tunneling behavior, which verifies PEI as a molecular link between CNT tips and silicon. The hierarchical structural level of carbon nanotube reinforcements was examined in [9].

Narrow-band luminescence was observed at the short-wavelength edge of the luminescence spectrum of polyethylene and polytetrafluoroethylene. The characteristics of this luminescence permit its assignment to the radiation emitted in recombination of ruptured C-C bonds in polymer chains [10]. The photoluminescence of polyethylenimine with carbon multiwall nanotubes on silicon structures was investigated in [11]. High photoluminescence intensity of composite was measured due to low non-radiative proton recombination on boundary microporous layer and "polymer-nanoparticle" nanocoating.

In this paper, we investigated the opportunities to enhance the properties of nanostructured surfaces "polymer-multiwall carbon nanotube" composites at 300 K. It was confirmed connection between the composite IR absorption at in the spectral area of sp^3 hybridization bonds and the primary amino group, $\gamma_w(\text{CH})$ and $\gamma_w(\text{CH}_2)$ vibrations. In addition, we measured IR reflectance maxima in the spectral

area of CH valence and deformation vibrations after formation of composite "polybutadiene-carbon nanotube". The IR peak dependencies on the CNT content at spectral area of sp^3 hybridization bonds are described by a 1D Gaussian curve for the diffusion equation in the electric field between electrons of nanotubes and protons in polymer. It determines the "semiconductor" n-p model to improve the strength properties of composite films of polyethylenimine, polyamide-6, and polypropylene with multiwall carbon nanotubes due to the composite structuring supported by vibrations in the intrinsic electric field.

2. Experimental

Carbon high purity multiwall nanotubes (CNTs) of 2 μm length and 20 nm diameter (Figure 1, a-b) were obtained by catalytic pyrolysis of unsaturated hydrocarbons [12].

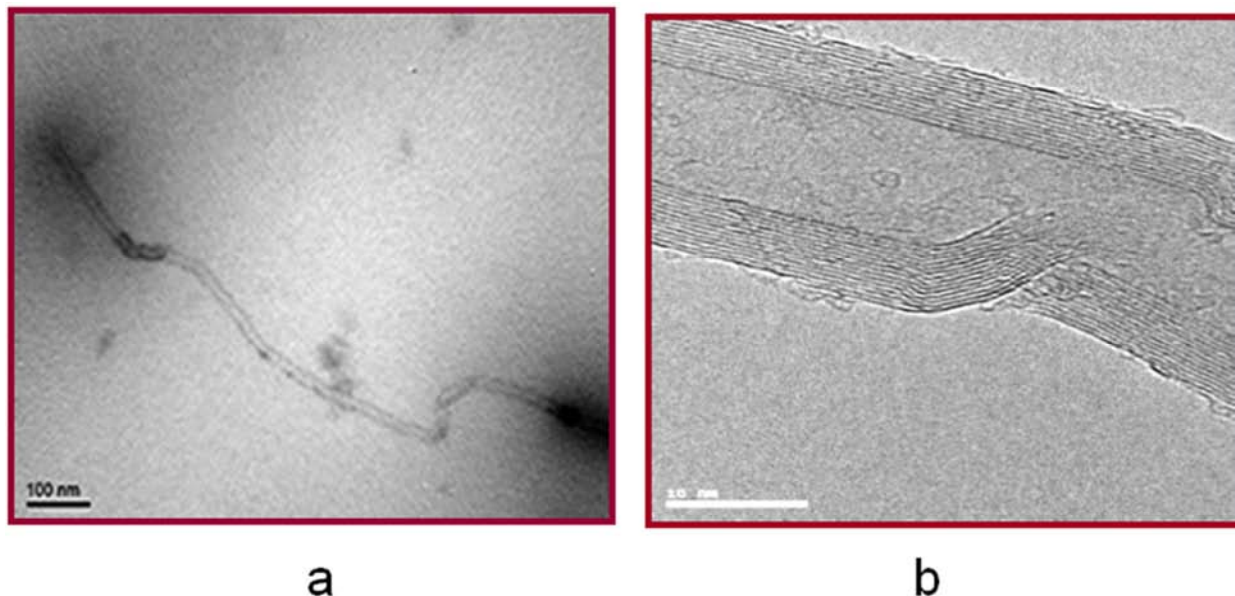


Figure 1. a) Morphology of carbon multiwall nanotube according to the AFM data; b) fragment of carbon multiwall nanotube.

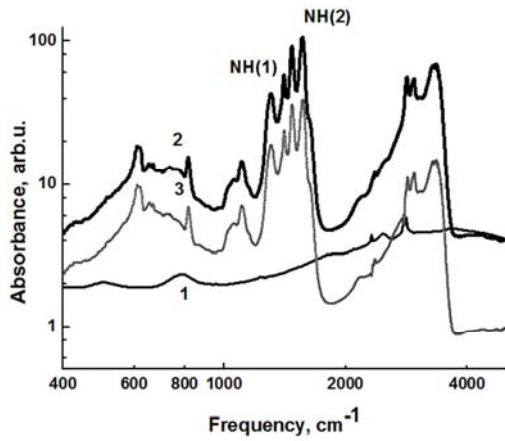
Nanoparticles morphology was investigated by the atomic force microscopy (AFM, NanoScope IIIa Dimension 3000TM). The composites were made of polyethylenimine, polyamide-6 and polypropylene filled by a mixture of CNTs with the polymer powder and dried. Composites were formed by hot pressing. Compression and tension tests of the polymeric materials and their composites were measured by tensile machine 2167-R50 with automatic recording of the deformation diagram. Thin polymeric films (100-150 μm thick) without and with CNTs were prepared out using Thermo HYDROPRESS for IR absorbance spectra measurement. Chemical states in composites were identified by IR absorption and reflectance spectra using a PerkinElmer Spectrum BXII IR Fourier spectrometer in the spectral range of 300-8000 cm^{-1} . The optical absorption spectra were measured at normal incidence of IR radiation on the sample at room temperature. In addition, we prepared powders of composites "polybutadiene-carbon nanotube" with KBr and

measured IR reflectance in the spectral area 300-4000 cm^{-1} .

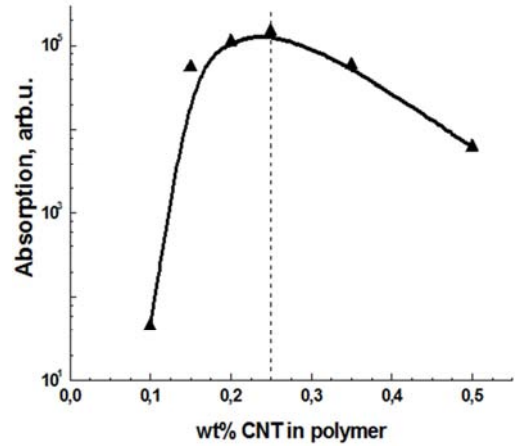
3. Results and Discussion

Figure 2a shows IR spectra of polyethylenimine (curve 1), the composite "polyethylenimine-carbon nanotubes" (curve 2) and the ratio of spectra 1 and 2 (curve 3). Figure 2b shows IR absorption by N-H(1) (curve 1) and N-H(2) (curve 2) bonds in composites based on polyethylenimine vs the carbon nanotube content in polymer.

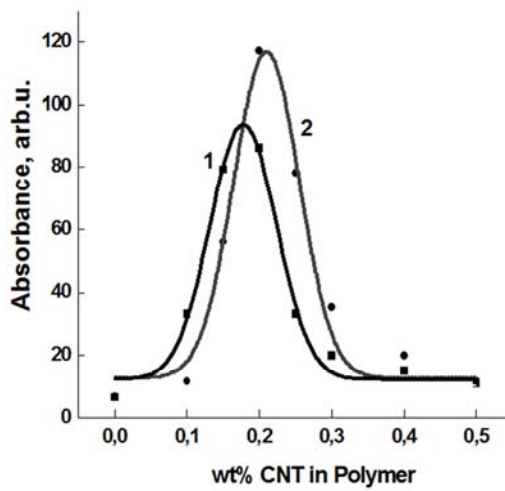
After formation of the "polyethylenimine-carbon nanotubes" composite intensive absorption maxima were measured in area of the sp^3 hybridization (D) bonds at the frequency of N-H(1) oscillations in the primary amino group of PEIs and in area of the sp^2 hybridization (G) bonds for the N-H(2) oscillation frequencies in secondary amino group of PEIs (Figure 2a and Figure 2b).



a)

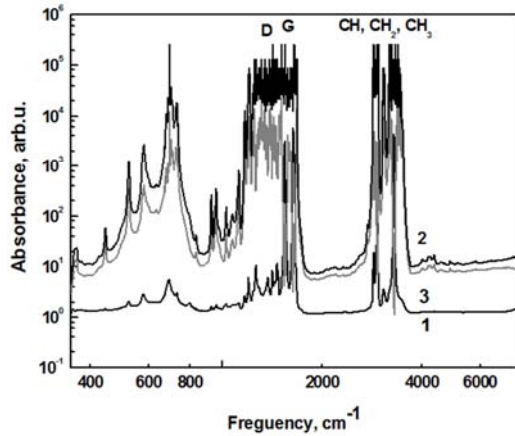


b)

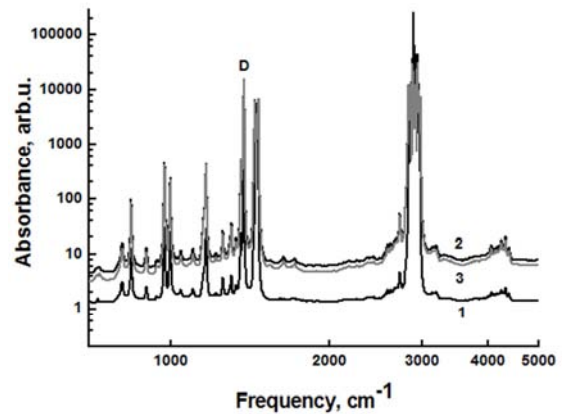


b)

Figure 2. a) IR spectra of polyethylenimine (curve 1), the composite "polyethylenimine-carbon nanotubes" (curve 2) and the ratio of spectra 1 and 2 (curve 3); b) IR absorption by N-H(1) (curve 1) and N-H(2) (curve 2) bonds in composites based on polyethylenimine vs the carbon nanotube content in polymer.



a)



a)

Figure 3. a) IR absorption spectra of polyamide (curve 1), "polyamide-carbon nanotubes" composite (curve 2) and the ratio of the curves 1 and 2 (curve 3); b) IR absorption at the frequencies of sp^3 hybridization bonds (D) in composites based on polyamide-6 vs the carbon nanotube content.

Figure 3a shows IR absorption spectra of polyamide (curve 1), "polyamide-carbon nanotubes" composite (curve 2) and the ratio of the curves 1 and 2 (curve 3).

After adding CNTs to polymers (concentration of 0.25%), IR absorption of "composite/polymer" films exceeds that of polymer films essentially. Higher C-C fluctuations, CH, CH₂ and CH₃ bond absorption correspond to higher IR absorption of composites at the frequencies of sp^3 hybridization bonds (Figure 3b).

After adding CNTs (concentration of 0.25%) to polypropylene (Figure 4a) IR absorption exceeds the absorption of polypropylene 4-8 times in all measured spectral range. This increases the intensity of the C-C bond vibrations (835 and 1000 cm^{-1}), as well as fluctuations $\delta(CH_3)$ – 1380 cm^{-1} , $\delta(CH_2)$ – 1440 cm^{-1} , $\delta_a(CH_3)$ – 1470 cm^{-1} [13, 14].

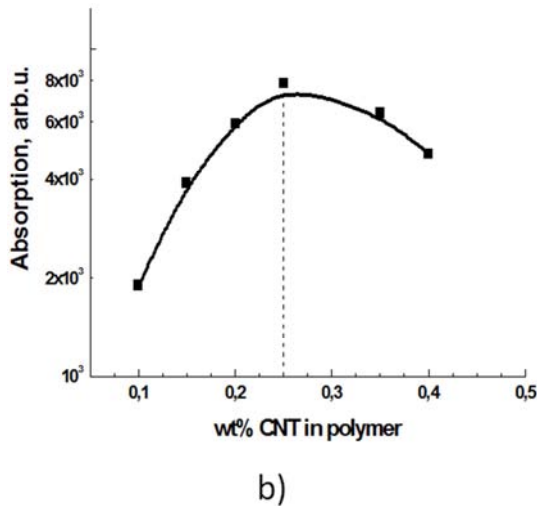


Figure 4. a) IR absorption spectra of polypropylene (curve 1), composite "polypropylene-carbon nanotubes" (curve 2) and the ratio of curves 1 and 2 (curve 3); b) IR absorption by sp^3 hybridization bonds (D) in composites based on polypropylene vs the carbon nanotube content in polymer.

After formation of the "polypropylene-carbon nanotubes" composite intensive absorption maxima were measured in area of the sp^3 hybridization (D) bonds at the frequency of $\gamma_{\omega}(\text{CH})$ vibrations (Figure 4b). Higher C-C fluctuations, CH, CH_2 and CH_3 bond absorption correspond to higher absorption of composites at the frequencies of sp^3 hybridization bonds.

IR reflectance maxima of composite "rubber-carbon nanotube" are measured at 2.5% CNTs (Figure 5a) in the area of CH deformation vibrations at frequencies 1297 cm^{-1} , 1466 cm^{-1} and 1728 cm^{-1} and valence vibrations at frequencies 2844 cm^{-1} and 2914 cm^{-1} [15].

Figure 5b shows dependences of relative IR reflectance R/R_0 of composite "polybutadiene rubber-carbon nanotube" on the carbon nanotube content in the area of CH_3 (curve 1, 2844 cm^{-1}) and CH_2 (curve 2, 2914 cm^{-1}) valence vibrations and relative tensile strength N/N_0 for two types of composites (curves 3-4).

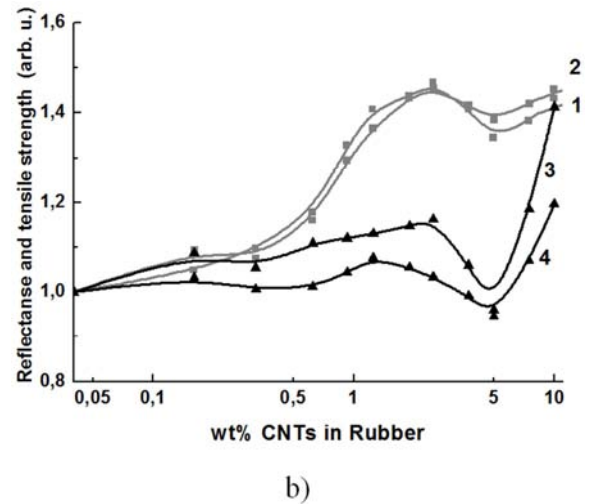
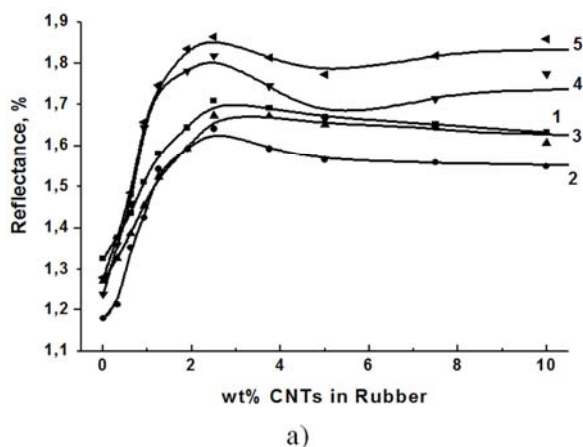


Figure 5. a) IR reflectance maxima of composite "rubber-carbon nanotube" vs the carbon nanotube content in polymer in the area of CH deformation vibrations (1 - 1297 cm^{-1} , 2 - 1466 cm^{-1} and 3 - 1728 cm^{-1}) and valence vibrations (4 - 2844 cm^{-1} , CH_3) and 5 - 2914 cm^{-1} , CH_2); b) relative IR reflectance R/R_0 in the area of CH_3 (curve 1) and CH_2 (curve 2) valence vibrations and the relative tensile strength N/N_0 for two types of composites "polybutadiene rubber-carbon nanotube" (curves 3-4) vs the carbon nanotube content in rubber.

There are maxima of dependences 1-4 from Figure 5b at 0.16, 1.25 and 2.5 wt% CNTs and pronounced minimum at 5 wt% CNTs. That minimum corresponds to minima IR reflectance of CH_3 and CH_2 valence vibrations. In addition, at high CNTs content ($> 5\text{ wt}\%$ CNTs) dependences 3 and 4 from Figure 5b became almost linear and proportional to CNTs surface in composite according to [8] and [18] results.

IR absorption in spectral area of sp^3 hybridization bonds in composites of polymers with multiwall carbon nanotubes has maxima (Figures 2b, 3b, 4b and 5) at its dependencies on CNT content. Thus, the maxima correspond to fixed distance between nanotubes. According to 2D model of CNTs distribution distance between nanotubes in composites depends on the CNTs concentration (N_{CNT}), its content (wt% CNT) and the nanotube volume (V_{CNT}):

$$a = (N_{\text{CNT}})^{-1/2} = (\% \text{ CNT}/100V_{\text{CNT}})^{-1/2} \quad (1)$$

The IR absorption maximum in area of sp^3 hybridization bonds (D) of composite polyethylenimine-carbon nanotubes (Figure 2b) corresponds to the average distance $a = 0.31\text{ }\mu\text{m}$ between the cylindrical CNT (diameter of 20 nm, length of 2 μm). The IR absorption maximum for sp^3 hybridization bonds (D) of composites polyamide-carbon nanotubes and polypropylene-carbon nanotubes (Figure 3b and Figure 4b) corresponds to the average distance $a = 0.35\text{ }\mu\text{m}$ between the cylindrical CNTs.

Obtained maxima one can explain by the geometric factor - characteristic volume around the cylindrical CNT at a distance of $a_m/2$ from nanotubes. As $a > a_m$, the characteristic volume around CNT increases due to increasing of the content of CNT - % CNT, N_{CNT} , IR absorption increases too. The characteristic volume around CNT and IR absorption decreases with growth of CNT content at $a < a_m$, Surface of

all nanotubes in composites S_{CNT} is proportional to the concentration of CNT (N_{CNT}) and have not peak in dependence on CNT content as in Figures 2b, 3b, 4b and 5.

Figure 6 shows the calculated (according to Equation (1)) dependences of average distance a between CNT (curve 1), geometric approximation (curve 2, characteristic volume around CNT), experimental dependence from Figure 4b of the IR absorption peak in area of sp^3 hybridization of "polypropylene-CNTs" composite on CNT content.

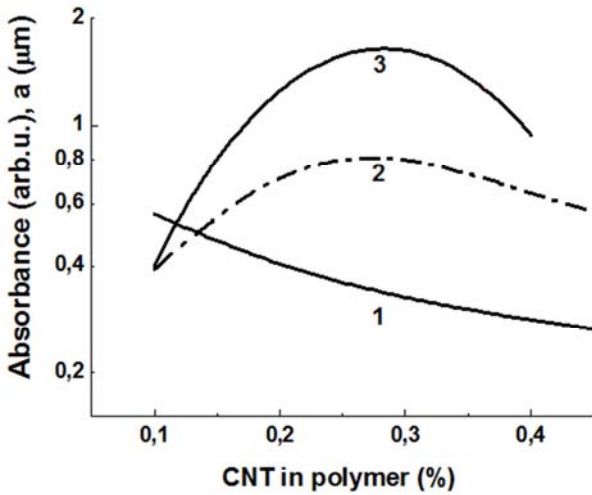


Figure 6. Dependences on CNTs content of: (1) average distance a between CNT; (2) geometric approximation – characteristic volume around CNT; (3) experimental dependence from Figure 4b.

The obtained geometric approximation (Figure 6, curve 2) explains qualitatively only the experimental dependence of IR absorption peak in bonds sp^3 hybridization (D) of "polypropylene-carbon nanotube" composite on the CNT content. This relationship is more nonlinear and has the form of a 1D Gaussian curve (Figure 6, curve 3), which corresponds to the diffusion equation in the electric field.

The intrinsic electric field between electrons of nanotubes and protons in polymer matrix is determined by band bending and has a space charge region (SCR) of width w (Figure 7).

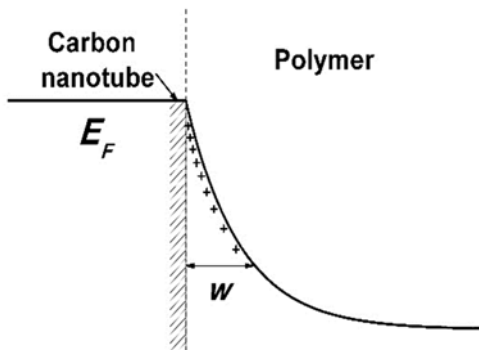


Figure 7. Band bending and SCR width w at the "polymer-CNTs" boundary.

To calculate the SCR width we used the Poisson equation in a cylindrical coordinate for system around a cylindrical

nanotube:

$$\frac{1}{r} \frac{\partial}{\partial r} \left(r \frac{\partial Y}{\partial r} \right) = - \frac{\rho_q}{\epsilon \epsilon_0 kT} \quad (2)$$

where: r - the radius vector, ρ_q - the charge density.

We used next the boundary conditions for the area of the SCR width w for a cylindrical nanotube with diameter d : $E(d/2 + w) = 0$, $Y(d/2 + w) = 0$, $Y(d/2) = Y_S$, where E is the electric field strength, Y_S - the value of the potential on the surface of the nanotube. Integrating Eq. (2) and using the above boundary conditions, we obtained next equation [16]:

$$\frac{16\epsilon\epsilon_0 Y_S w}{eq_v d^2} - 1 + \left(1 + \frac{2w}{d}\right)^2 \left(1 - 2 \ln\left(1 + \frac{2w}{d}\right)\right) = 0 \quad (3)$$

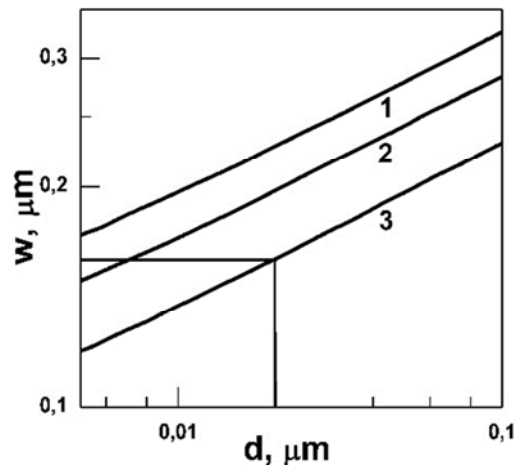


Figure 8. Dependence of SCR width w around cylindrical nanotubes on their diameters for surface potential Y_S : 1) $-12 kT$; 2) $-8 kT$; 3) $-4 kT$.

Figure 8 shows dependences of the size of the space charge region of cylindrical nanotubes calculated from Eq. (3) on their diameter at various values of the surface potential. The SCR width w decreases with the diameter of nanotubes decrease (Figure 8). The length $a = 310$ nm between cylindrical CNT corresponds to the distance between nanotubes $w = (a_m - d)/2 = 155$ nm in composite "polyethylenimine-carbon nanotubes" for maximum of IR absorption (Figure 2b) and surface potential $Y_S = -3kT$ (79.5 mV) and electric field intensity $E = Y_S/w = 5.12 \cdot 10^3$ V/cm. The length $a = 35$ nm between cylindrical CNT corresponds to the distance between nanotubes $w = (a_m - d)/2 = 170$ nm in composites "polyamide-carbon nanotubes" and "polypropylene-carbon nanotubes" (Figure 3b and Figure 4b) for maximum of IR absorption. It corresponds to surface potential $Y_S = -4kT$ (106 mV) (Figure 8), electric field intensity $E = Y_S/w = 6.3 \cdot 10^3$ V/cm for $w = 170$ nm between cylindrical CNTs (diameter of 20 nm, length of 2 μ m) at maximum at IR absorption peak in area of bonds of sp^3 hybridization (D).

Carbon nanotubes divided into two main groups: (1) the molecular associated nanotubes linked through weak short-acting interactions, van-der-Waals forces, and (2) nanotubes with additional strong covalent sp^3 type C-C

bonding for long-acting interactions.

The recent advances in both the production and characterization of composites “polymer-CNTs” for first case enabled the expansion of composite reinforcement levels to the nanometer scales of short-acting interactions [8]. Molecular dynamics simulations demonstrate the formation of an ordered layer of polymer matrix surrounding the nanotube [18]. This thin layer, known as the interphase, not determines at low (0.1-0.5) % CNTs concentration the overall mechanical response of the composite as the only reinforcement phase. But at high CNTs content (> 5 % CNTs) dependences for tensile strength became almost linear and proportional to CNTs surface in composite according to [8] and [18] results.

For second case, the way to improve the strength properties of composites “polymer-CNTs” is the polymer crystallization [17]. For the long-acting hundreds nanometer interactions, the polymer crystallization depends on sp^3 C-C bonds organization in the intrinsic electric field according to “semiconductor” n-p model. As a result, the profile analysis of X-ray reflexes confirmed high crystallinity degree of investigated “polymer-CNTs” composites - from 72% to 85% [17]. Crystalline polymers demonstrate high tensile strength (30-40 MPa for composite “polyamide 6-CNTs”).

4. Conclusion

IR absorption maxima is measured after formation of composite “polyethylenimine-carbon nanotube” in the area of the sp^3 hybridization bonds at the frequency of primary amino groups of polyethylenimine. High IR absorption at frequencies of sp^3 hybridization bonds of polypropylene, polyamide-6 with carbon nanotubes is determined by $\gamma_{\omega}(\text{CH})$ and $\gamma_{\omega}(\text{CH}_2)$ vibrations. We evaluated IR reflectance maxima in the area of CH valence and deformation vibrations after formation of composite “polybutadiene rubber-carbon nanotube”. The IR peak dependencies on the carbon nanotube content is described by a 1D Gaussian curve for the diffusion equation in the electric field. It determines the “semiconductor” p-n model to improve the strength properties during formation of polyethylenimine, polyamide and polypropylene composites with multiwall carbon nanotubes. According to this model the composite crystallization enhanced by the vibration bonds in the intrinsic electric field between electrons of nanotubes and protons in polymer. Tensile strength for polyamide-6 composites at 0.25% CNT increases 1.7 times and tensile deformation – 2.3 times. Surface of all nanotubes in composites is proportional to the concentration of CNTs and have not peak in dependence on CNTs content.

Acknowledgements

Acknowledgements for this work support by the Project of Scientific and Technical Cooperation between the National Academy of Sciences of Ukraine and the Ningbo University of Technology (China).

References

- [1] M. Treacy, T. Ebbesen, and J. Gibson “Exceptionally high Young’s modulus observed for individual carbon nanotubes”, *Nature*, 1996, vol. 381, pp. 678-683.
- [2] L. Bokobza, “Multiwall carbon nanotube elastomeric composites”, *Polymer*, 2007, vol. 48, pp. 4907-4911.
- [3] W. Bauhofer, and J. Kovacs “A review and analysis of electrical percolation in carbon nanotube polymer composites”, *Comp. Sci. Technol.* 2009, vol. 69, pp. 1486-1491.
- [4] L. Lacerda, A. Bianco, M. Prato, and M. Kostarelos “Carbon nanotubes as nanomedicines: from toxicology to pharmacology”, *Adv. Drug Del. Rev.* 2006, vol. 58, pp. 1460-1463.
- [5] M. Wilder, L. Venema, A. Rinzler, R. Smalley, and C. Dekker, “Electronic structure of atomically resolved carbon nanotubes”, *Nature*, 1998, vol. 391, pp. 59-65.
- [6] S. Fan, M. Chapline, N. Franklin, T. Tombler, A. Cassell, and H. Dai “Self-oriented regular arrays of carbon nanotubes and their field emission properties”, *Science*, 1999, vol. 283, pp. 512-517.
- [7] B. Wei, R. Vajtai, and P. Ajayan, “Reliability and current carrying capacity of carbon nanotubes”, *Appl. Phys. Lett.*, 2001, vol. 79, pp. 1172-1178.
- [8] G. Zou, H. Yang, M. Jain, H. Zhou, D. Williams, M. Zhou, T. McCleskey, A. Burrell, and Q. Jia, “Vertical connection of carbon nanotubes to silicon at room temperature using a chemical route”, *Carbon*, 2009, vol. 47, pp. 933-937.
- [9] E. Thostenson, Z. Ren, and T-W. Chou, “Advances in the Science and Technology of Carbon Nanotubes and their Composites”, *A Review. Composites Science and Technology*, 2001, vol. 61, pp. 1899-1905.
- [10] M. Kompan, and I. Aksyanov, “Near-UV narrow-band luminescence of polyethylene and polytetrafluoroethylene”, *Phys. Solid State*, 2009, vol. 51, pp. 1083-1090.
- [11] L. Karachevtseva, M. Kartel, O. Lytvynenko, V. Onyshchenko, K. Parshyn, and O. Stronska, “Formation of carbon sp^3 hybridization bonds in local electric fields of composites “polymer-CNT”, *Advanced Materials Letters*, 2017, vol. 8, pp. 322-326.
- [12] K. Awasthi, A. Srivastava, and O. Srivastava, “Synthesis of Carbon Nanotubes”, *J. Nanosci. Nanotech.*, 2005, vol. 5, pp. 1616-1620.
- [13] S. Krimm, *Infrared Spectra of High Polymers*, *Fortschr. Hochpolym.-Forsch.*, 1960, p. 172.
- [14] A. Miyake, “Infrared spectra and crystal structures of polyamide”, *Polymer Chemistry*, 1960, vol. 44, pp. 223-232.
- [15] W. C. Sears “Infra-Red Spectra of Rubber and High Polymers”, *Rubber Chemistry and Technology*, 1941, vol. 14, pp. 572-579.
- [16] V. Onyshchenko, and L. Karachevtseva, “Conductivity and photoconductivity of two-dimensional macroporous silicon structures”, *Ukrainian J. Phys.*, 2013. vol. 58, pp. 846-850.

- [17] N. Resanova, M. Kartel, Yu. Sementsov, G. Prikhod'ko, I. Melnik, and M. Tsebrenko, "Rheological Properties of Molten Mixtures of Polypropylene/Copolyamide/Carbon Nanotubes", *Chemistry, Physics and Technology of Surface*, 2011, vol. 2, pp. 451-458.
- [18] M. Malagù, M. Goudarzi, A. Lyulin, E. Benvenuti, and A. Simone, "Diameter-dependent elastic properties of carbon nanotube-polymer composites: Emergence of size effects from atomistic-scale simulations", *Composites Part B: Engineering*, 2017, vol. 131, pp. 260–281.